On the importance of Ni–Au–Ga interdiffusion in the formation of a Ni–Au/p-GaN ohmic contact

Jules Duraz, Hassen Souissi, Maksym Gromovyi, David Troadec, Téo Baptiste, Géraldine Hallais, Nathaniel Findling, Phuong Vuong, Rajat Gujrati, Thi May Tran, et al.

Journal of Applied Physics

RESEARCH ARTICLE | JANUARY 08 2026

On the importance of Ni–Au–Ga interdiffusion in the formation of a Ni–Au/p-GaN ohmic contact

Jules Duraz ; Hassen Souissi ; Maksym Gromovyi ; David Troadec; Téo Baptiste ; Géraldine Hallais ; Nathaniel Findling; Phuong Vuong; Rajat Gujrati; Thi May Tran ; Jean-Paul Salvestrini ; Maria Tchernycheva ; Suresh Sundaram ; Abdallah Ougazzaden ; Gilles Patriarche ; Sophie Bouchoule

J. Appl. Phys. 139, 025102 (2026)
https://doi.org/10.1063/5.0295857

Journal of Applied Physics ARTICLE pubs.aip.org/aip/jap

On the importance of Ni–Au–Ga interdiffusion in the formation of a Ni–Au/p-GaN ohmic contact

Cite as: J. Appl. Phys. 139, 025102 (2026); doi: 10.1063/5.0295857
Submitted: 11 August 2025 · Accepted: 12 December 2025 ·
Published Online: 8 January 2026

Jules Duraz,[1] Hassen Souissi,[1] Maksym Gromovyi,[1,a)] David Troadec,[2] Téo Baptiste,[1] Géraldine Hallais,[1] Nathaniel Findling,[1] Phuong Vuong,[3] Rajat Gujrati,[3] Thi May Tran,[3] Jean-Paul Salvestrini,[3,4] Maria Tchernycheva,[1] Suresh Sundaram,[3] Abdallah Ougazzaden,[3,4] Gilles Patriarche,[1] and Sophie Bouchoule[1,b)]

AFFILIATIONS

[1]Centre de Nanosciences et de Nanotechnologies, C2N, UMR 9001, CNRS, Université Paris-Saclay, 91120 Palaiseau, France
[2]Institut d'Electronique, de Microélectronique et de Nanotechnologie, IEMN, UMR 8520, CNRS, Université de Lille, 59652 Villeneuve d'Ascq, France
[3]Georgia Tech CNRS, IRL 2958, GT-Europe, 57070 Metz, France
[4]School of Electrical and Computer Engineering, Georgia Institute of Technology, Atlanta, Georgia 30332-0250, USA

[1)]**Present address:** CRHEA, UMR7073, CNRS, Université Côte d'Azur, 06 560 Valbonne, France.
[b)]**Author to whom correspondence should be addressed:** sophie.bouchoule@cnrs.fr

ABSTRACT

High-resolution transmission electron microscopy (TEM) coupled to energy dispersive X-ray spectroscopy (EDX) is used to clarify the exact role of Ni–Au–Ga interdiffusion mechanisms taking place during rapid thermal annealing under an oxygen atmosphere of a Ni–Au/p-GaN contact. It is shown that oxygen-assisted, Ni diffusion to the top surface of the metallic contact through the formation of a nickel oxide (NiO_x) is accompanied by Au diffusion down to the GaN surface and by Ga out-diffusion through the GaN/metal interface. Electrical characterizations of the contact by a transmission line method show that an ohmic contact is obtained as soon as a thin, Au–Ga interfacial layer is formed, even after complete diffusion of Ni or NiO_x to the top surface of the contact. Our results clarify that the presence of Ni or NiO_x at the interface is not the main origin of the ohmic-like behavior in such contacts. Auto-cleaning of the interface during the interdiffusion process may play a role, but TEM-EDX analysis evidences that the creation of Ga vacancies associated with the formation of a Ga–Au interfacial layer is crucial for reducing the Schottky barrier height and maximizing the amount of current flowing through the contact.

I. INTRODUCTION

GaN and related group III-nitride semiconductors are now widely used for the fabrication of opto-electronic devices, such as transistors for high-power, high-temperature applications,[1] semiconductor lasers, and light-emitting diodes (LEDs) in the visible-to-UV spectral range.[2] In such devices, the main limiting factor in performance is the poor quality of the ohmic contact on the p-side of the diode.[3] Indeed, the implementation of a low-resistive contact metallization scheme for p-GaN has represented a challenge in the past decades due to the large activation energy of a p-type dopant, such as Mg (∼160–200 meV),[4] and hence low density of ionized acceptors typically of at most $\sim 10^{18}\,cm^3$,[4] but also due to the lack of metals with a work function adapted to that of p-GaN (∼6.6 eV),[3] required to minimize the barrier height of the metal/semiconductor Schottky diode.[5,6] A comprehensive analysis of the behavior of metal/p-GaN contacts has also been complicated by variations in the growth conditions and device fabrication methods, including the control of the GaN/metal interface, leading to important variations in the Fermi level pinning effect, impacting the electrical performance of the contact.[6,7] Nevertheless, high-work-function (∼5 eV) metals, such as Ni, Au, Pt, and Pd, have been mostly studied in order to minimize the Schottky barrier height and to achieve an ohmic behavior.[4,8–12] Thermal annealing of Ni–Au/p-GaN contact was first investigated to reduce the

specific contact resistance,[13] and a beneficial effect of annealing under an oxygen-containing atmosphere was discovered,[14,15] attributed to the formation of a NiO/p-GaN interface.[14,16] However, other works concluded that NiO was not the reason for the Ni–Au metallization to yield ohmic behavior after thermal annealing in an oxidizing atmosphere.[17] Other effects were, thus, emphasized to explain the ohmic-like behavior after annealing, namely, the removal of surface contamination and native oxide during Ni/Au layer reversal,[9,18,19] or the creation of Ga vacancies in p-GaN close to the metal interface.[20–22] Some authors also pointed out the formation of a (Ni–)Au–Ga alloy in contact with p-GaN,[18,20–22] possibly involved in the reduction of the Schottky barrier height. However, the exact role and relative importance of the different mechanisms have not been clarified yet. In a recent experimental study, using TEM coupled with energy dispersive X-ray spectroscopy (EDX) analysis, it was again supposed that the creation of Ga vacancies may play a role, but the presence of a NiO/p-GaN interface was inferred to have a major importance in the formation of an ohmic contact.[23] This latter conclusion differs from a previous qualitative TEM-EDX analysis by Greco *et al.*,[4,24] showing that the formation of NiO_x cannot explain the reduction of the contact resistance after O_2-annealing. On the other hand, Greco *et al.* evidenced Au–Ni interdiffusion, but did not investigate Ga diffusion.[24]

We have conducted a detailed TEM-EDX study attempting to elucidate the exact role of Ni/NiO_x, Au, or (Ni–)Au–Ga alloy in contact with p-GaN in the formation of an ohmic-like p-GaN contact, and to clarify the importance of the different diffusion processes assisted by thermal annealing under an oxygen atmosphere. Using the same epitaxial structure, we have compared the electrical performance of the p-GaN/Ni–Au contact for different annealing conditions and metal evaporation conditions. We systematically correlated the electrical results with high-resolution TEM coupled to EDX analysis. We conclude that, in our processing conditions, the creation of Ga vacancies during Ni–Au/Ga interdiffusion processes plays the major role in the reduction of the Schottky barrier height.

II. EXPERIMENTAL CONDITIONS AND METHODS

Briefly, the InGaN/GaN blue LED MQW heterostructure used for the study is grown by MOCVD and schematically depicted in Fig. 1. The p-GaN top surface is terminated by a 12 nm thick p^+-GaN surface layer with an active dopant concentration up to $3 \times 10^{17}\,cm^{-3}$.

TLM patterns used for the electrical characterization of the p-GaN/metal contacts[25] are defined by optical lithography and a standard metal lift-off process. A chemical cleaning step is first carried out prior to the photolithography step. An *ex situ* deoxidation sequence based on HCl and HF is then applied prior to metal evaporation. It was observed separately from *ex situ* XPS analysis that this chemical deoxidation sequence minimized the amount of native gallium oxide (GaO_x) at the GaN surface, for which residual thickness was estimated to be lower than ~0.3 nm within 10 min following the deoxidation. The sample is then immediately installed into the loadlock of the electron-beam vacuum evaporator, and a 20 nm thick Ni layer and a 200 nm thick Au top layer are deposited

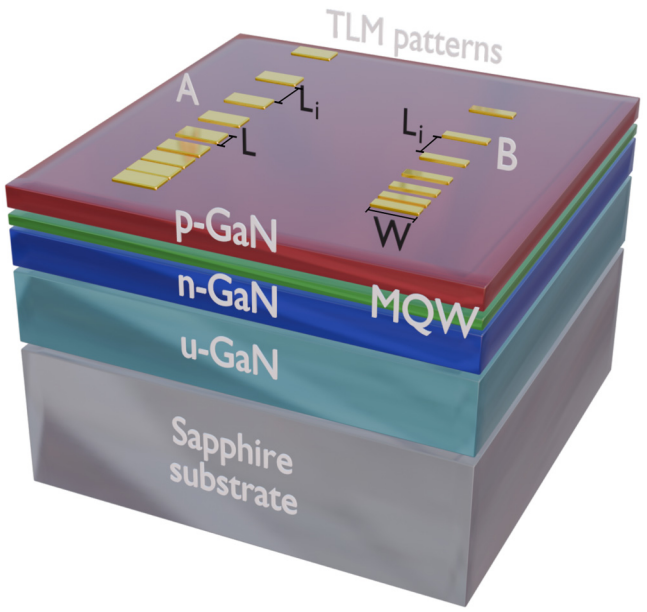

FIG. 1. Schematics of the epitaxial structure used for the study and geometry of the transmission line method (TLM) pads used for the electrical characterization of the contact. Pad dimensions (W and L) and spacing (L_i) can be found in the supplementary material.

at a constant evaporation rate of 0.5 nm/s, regulated by a quartz oscillator.

Rapid thermal annealing (RTA) of the contacts is always performed at atmospheric pressure under pure oxygen ambient, unless explicitly specified in the following. The annealing temperature is generally fixed to 450 °C, for annealing times varied from 2 to 10 min in the experiments, except for tests performed at 350 °C and up to 650 °C.

Two-probe measurements are performed in the [−5 V; +5 V] voltage range to retrieve the I–V characteristic between two successive TLM pads, depicted in Fig. 1. From these measurements, the specific contact resistance r_c is deduced by following the TLM method.[25] An estimate of the Schottky barrier height, Φ_B, is obtained according to the method used by Mori *et al.*[26] or Wahid *et al.*[7] The current I_{max} flowing between two TLM pads separated by distance $L_i = 20\,\mu m$, at a voltage difference set to 5 V, is given as a complementary figure of merit, practically considered the most relevant parameter for LED or laser diode applications.[27] The values of r_c, I_{max}, and Φ_B are listed in Table I for each sample of this study. For comparison purposes, the TLM I–V characteristics of the different samples are exemplified for fixed distance $L_i = 20\,\mu m$ in the following.

After electrical characterization, a TEM slice with a typical width of 15 μm and a height of 3 μm is taken from a TLM pad by Ga-Focused-Ion-Beam (FIB) etching for further physico-chemical and structural analyses of the GaN–metal stack and GaN/metal interfacial layer. Thin windows in the TEM slice are preferentially used for high-resolution TEM (HR-TEM) observations, while

TABLE I. Summary of electrical results for samples with different Ni/Au thickness and annealing conditions.

Sample	Ni/Au thickness (nm/nm)[a]	Annealing conditions (°C, ∅, min)	I_{max} (mA)	Φ_B (eV)	r_c (Ω cm^2)
A	20/200	No annealing	0.27	0.68	1.4×10^{-1}
B	20/200	450 °C, O_2, 2 min	0.78	0.53	1.2×10^{-2}
C	20/200	450 °C, O_2, 10 min	0.98	0.49	6.6×10^{-3}
D	3/3	No annealing	0.60	0.56	1.3×10^{-2}
E	3/3	450 °C, O_2, 2 min	0.99	0.47[b]	1.0×10^{-2}
F	3/3 + 20/50[c]	650 °C, O_2, 2 min	0.85	0.50	1.9×10^{-2}
G	3/3	350 °C, O_2, 2 min	0.70	0.51	2.3×10^{-2}
H	3/3	350 °C, O_2, 10 min	0.88	0.47[b]	3.0×10^{-2}

[a]The evaporation rates for the thick (Ni/Au 20/200 nm) and thin (Ni/Au 3/3 nm) metal layers are 0.5 and 0.1 nm/s, respectively.
[b]Assuming the applicability of the thermoionic emission carrier transport model.
[c]A second Ni–Au evaporation on the TLM pads subsequent to thermal annealing has been carried out on sample F to allow for the electrical measurements.

thicker ones are preferentially used for TEM-EDX analysis. EDX coupled with TEM allows for the estimation of the atomic composition of the analyzed area in different ways. First, 2D cartographies of the relative distribution of the different atoms present in the analyzed area can be reconstructed, referred to as an EDX map in the following. Second, a quantitative estimation of the local composition in atomic percentage can be estimated from the EDX spectra: the relative compositional profile can be calculated, at several points along a linescan defined perpendicular to the layer interfaces, leading to a compositional profile. For the third alternative, several rectangular zones can be manually selected in homogeneous regions of the analyzed area, and the quantitative, average composition in atomic percentage can be calculated in each zone independently.

Detailed information regarding the epitaxial structure, processing steps, electrical characterization, FIB etching, and TEM-EDX analysis, including a discussion about precision and uncertainties in the material composition, can be found in the supplementary material.

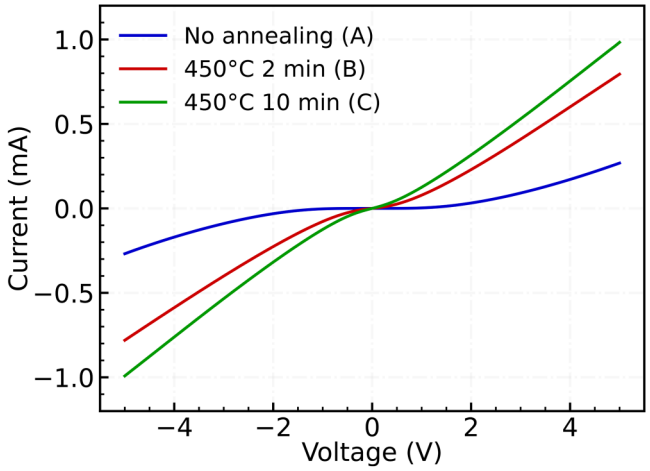

FIG. 2. TLM I–V characteristics measured for a distance between pads $L_i = 20\,\mu$m without annealing (blue), after annealing for 2 min (red), and after annealing for 10 min (green). Labels A–C refer to Table I.

III. RESULTS AND ANALYSIS

Figure 2 shows the TLM I–V curve of the non-annealed sample (A), for a distance between TLM pads $L_i = 20\,\mu$m. A Schottky barrier is clearly apparent, estimated to be of ∼0.70 eV in height as reported in Table I, and a rather low I_{max} value of 0.27 mA is reached at 5 V. The specific contact resistance value is found to be $r_c \sim 1.5 \times 10^{-1}\,\Omega\,\text{cm}^2$. The I–V curve presents a more ohmic-like profile after RTA for 2 min at 450 °C under an O_2 atmosphere (sample B). The I_{max} value is notably increased (to ∼0.80 mA), associated with the reduction of Schottky barrier height, and the specific contact resistance is decreased down to $1.2 \times 10^{-2}\,\Omega\text{cm}^2$. A longer annealing time of 10 min slightly improves the results; however, I_{max} tends to saturate to ∼1 mA, and r_c is only moderately reduced (down to $6.6 \times 10^{-3}\,\Omega\text{cm}^2$, sample C).

TEM-EDX analyses have been carried out for the non-annealed sample as well as after annealing for 2 and 10 min, respectively. Figure 3(a) shows a High-Angle Annular Dark-Field (HAADF) HR-STEM image of the GaN/Ni/Au stack for the non-annealed sample A. The thickness of the Ni/Au layers is measured to be approximately equal to the nominal thickness of 20/200 nm. It is observed that the starting of Ni deposition on the GaN surface is not completely uniform, with nano-grains formed in the Ni layer, leading to a rms surface roughness of ∼1.4 nm, estimated from the analysis of the HAADF image Z-contrast, assuming a Gaussian distribution.

The 200-nm thick gold layer also shows some larger nano-grains, leading to an estimated top surface rms roughness of ∼2 nm in the image. The GaN/Ni interface shows a lower intensity on the HAADF-STEM image, which may be interpreted either as nano-voids embedded in the TEM slice thickness or as the presence of a lighter material, presumably an oxide. The average thickness of this interfacial region is estimated to be 2.9 nm, from the analysis of the average Z-contrast in the HAADF-STEM image of Fig. 3(a). A quantitative analysis of the average atomic composition of the interfacial layer is performed in the selected zone labeled as 2 in Fig. 3(b). Ga,

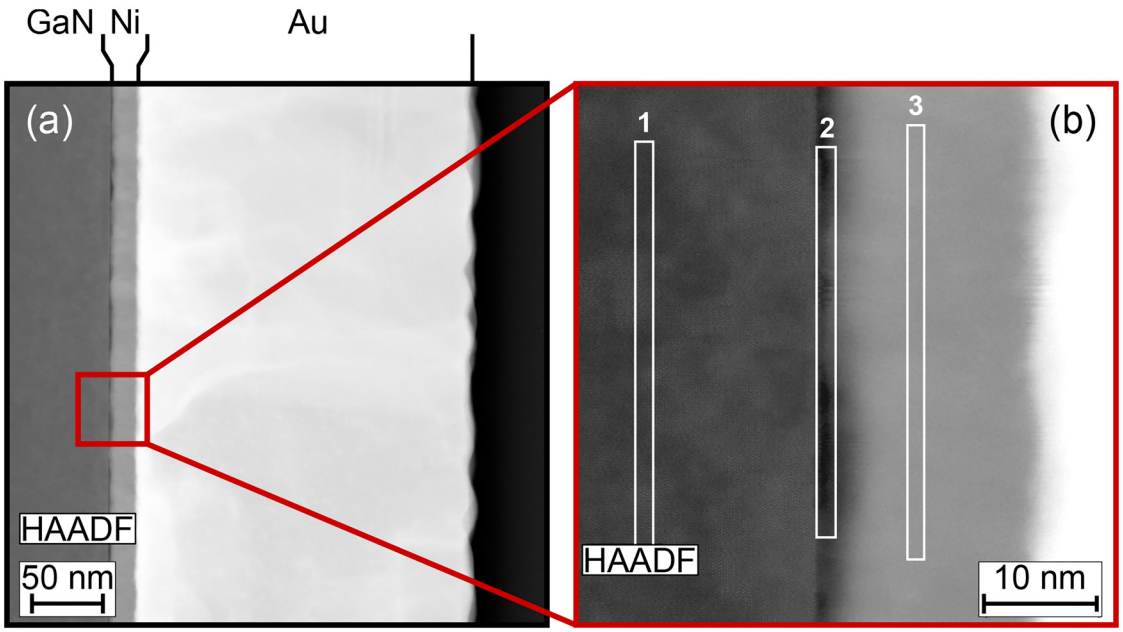

FIG. 3. Sample A (thick metal layers, non-annealed): (a) HAADF-STEM image of the GaN–Ni–Au stack and (b) an image of the region marked with a red square in (a). The three white rectangles in (b) correspond to the zones used to quantify the average composition in Table II.

N, Ni, and O can be detected in the average EDX spectrum, while Au is not detected. The atomic composition of the interface is compared to that of zones labeled as 1 and 3 in the GaN (∼15 nm below the GaN/Ni interface) and Ni (∼8 nm above the interface) layers, respectively. The results are listed in Table II. A 50/50 GaN stoichiometry is reasonably retrieved in zone 1, with the presence of a low amount of oxygen, close to the noise level (∼1–3%); as discussed in the supplementary material, this signal probably originates from the native gallium oxide at the TEM slice facets. Ni oxidation is much less pronounced in zone 3, with the oxygen signal close to the noise level in the corresponding average EDX spectrum, not shown. Again, this oxygen level may originate from Ga oxidation (from FIB) and also easy Ni oxidation at the TEM slice facets. Almost no trace of Au, nor of Ga, can be found in the 20 nm thick Ni layer, which acts as a diffusion barrier. The Ga atomic percentage of 1.7% is very close to the ∼2% value retrieved and attributed to Ga FIB pollution at the slice facets.

TABLE II. Average composition for sample A—Thick metal layers, non-annealed (HAADF TEM image: Fig. 3).

	Average atomic % in each zone[a]		
Elements	1 (GaN)	2 (interfacial)	3 (Ni)
Ga	50.6	47.4	1.7
N	47.9	3.9	0[b]
Ni	0.3[c]	40.2	94.3
O	1.3[d]	8.5	4.0

[a]The TEM slice thickness is fixed to 200 nm and the average material density to 5 (1), 6 (2), and 8 g/cm^3 (3).
[c]Ni is only present as traces and close to the spectrum background level.
[d]O percentage may vary from ∼1% to ∼3% depending on the selected area in the GaN bulk.
[b]Calculated value, no N signal in the EDX spectrum.

In contrast with zones 1 and 3, a more important oxidation can be measured in the interfacial layer (zone 2), with an oxygen percentage of 8.5% ± 1%. The interfacial layer, therefore, corresponds to a presumably discontinuous, $GaNiO_x$ layer. It may explain the presence of the Schottky barrier observed in Fig. 2 and Table I, but may also induce some Fermi level pinning effect impacting the effective Schottky barrier height.[7,27]

Figure 4(a) shows a large-view, Bright-Field (BF) HR-STEM image of the GaN/Ni/Au layers after RTA for 2 min at 450 °C in O_2 ambient (sample B). The structure of the initial Ni layer is strongly modified by the annealing, with the creation of polycrystalline nano-domains of high and low intensity, to be interpreted as low-density and high-density materials, respectively. Figure 4(b) corresponds to the EDX map of a high-intensity area marked with a green dashed square in Fig. 4(a). Ni is still present; however, Au interdiffusion in Ni is taking place through channels that may be related to the nano-grain boundaries in the initial Ni layer. Moreover, some Au accumulation is apparent within ∼2–3 nm right above the GaN surface. Figure 4(c) corresponds to the EDX map of a low-intensity area marked with a blue dashed square in Fig. 4(a). Au interdiffusion is much more pronounced in this area, which is consistent with a higher-density metallic alloy. Traces of Ga (signal above the Ga K-line noise level in the EDX spectrum)

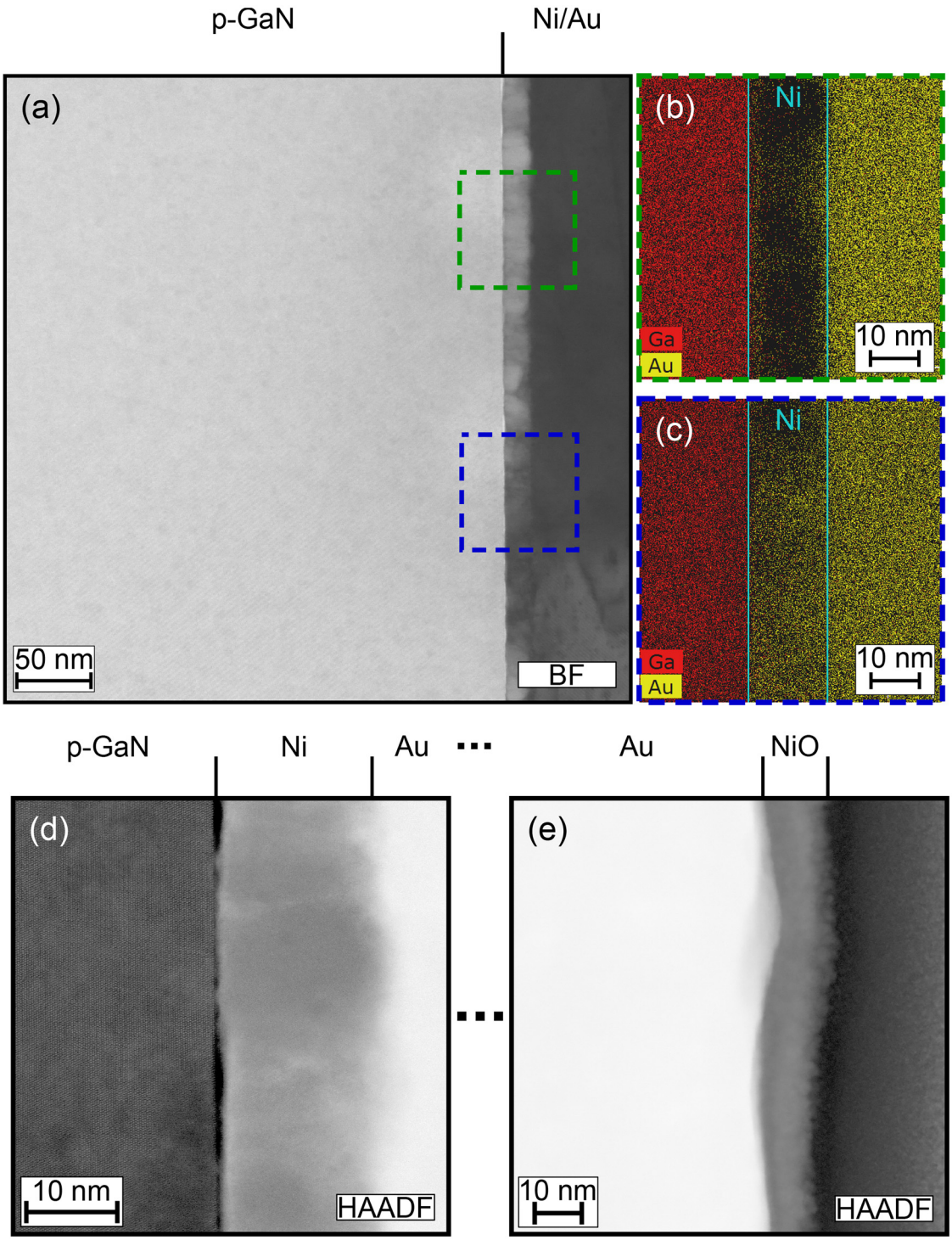

FIG. 4. Sample B (thick metal layers, annealed 2 min at 450 °C)—HR-STEM images and EDX mapping showing the relative distribution of Au and Ga atoms. (a) Large-view, Bright-Field (BF) STEM image of the p-GaN/Ni/Au stack. (b) EDX map in a region where Au interdiffusion is moderate. (c) EDX map in a region where Au interdiffusion is strong. (d) HAADF HR-STEM image at high magnification of the GaN/Ni/Au layers. (e) HAADF HR-STEM image at high magnification of the Au/NiO_x top surface. The cyan vertical lines in (b) and (c) are guides to the eye to locate the position of the as-evaporated Ni layer.

are also detectable in the initial Ni layer, as well as in the initial Au layer, on the EDX maps; however, quantitative analysis of the atomic composition is required to evaluate more precisely the importance of Ga diffusion. Figure 4(d) shows a high-magnification, HAADF HR-STEM image of the GaN/Ni/Au stack. The Z-contrast evidences that the low-density $GaNiO_x$ interfacial region detected before annealing is still present, but restricted to some discontinuous areas (dark areas) at the nano-scale. The channels of Au diffusion into the initial Ni layer can also be identified in the Z-contrast HAADF image, as brighter zones in the layer. As a first conclusion, the reduction of the Schottky barrier height observed in Fig. 2 after annealing for 2 min may be associated with the diffusion processes taking place in Fig. 4. As previously introduced, three physical effects may be involved: first, a reconstruction or "auto-cleaning" of the GaN/metal interface occurring during the interdiffusion[9,18,19] removing impurities and reducing the thickness of the native GaO_x oxide; second, the presence of Au close to the GaN surface, and presumably of a (Ni–)Ga–Au alloy formed with the observed Ga diffusion in the metallic layer,[18,21,22] leaving Ga vacancies at the GaN surface;[20–22] and third, the presence of a NiO_x layer in contact with the GaN surface.[14,16,23]

Figure 4(e) shows a HAADF HR-STEM image of the top surface at high magnification. A NiO_x layer has been formed almost everywhere on top of Au, as deduced from the EDX map and analysis shown in Table III. The average composition in atomic percentage can be calculated with the same approach as that used in Fig. 3(b). Table III summarizes the results obtained for several rectangular zones selected in the EDX maps associated with Figs. 4(b), 4(c), and 4(e), corresponding to the GaN/Ni/Au stack with moderate Au interdiffusion, the GaN/Ni/Au stack with strong Au interdiffusion, and the top Au/NiO_x layer, respectively. The quantitative analysis shows that the top amorphous NiO_x layer is oxygen-rich with a retrieved Ni/O ratio close to 40/60. The top part of the initial Au layer remains mainly composed of gold (95% in atomic percentage), and Ni is almost not present, consistent with fast Ni out-diffusion and accumulation at the surface after oxidation. The Ga traces in these zones can be attributed to Ga FIB pollution at the slice facets. The quantitative analysis in zones 4 and 8 in the EDX maps shows that the bottom part of the Au layer close to the initial Ni/Au interface also contains a moderate amount of Ni (6%), while traces of Ga may be attributed to FIB pollution.

The main effect of the thermal annealing can be observed in the initial Ni layer; its composition is non-uniform, as already evidenced by the Z-contrast HAADF-STEM images and EDX maps in Figs. 4(a)–4(c). In regions, such as that of Fig. 4(b), where Au diffusion into the Ni initial layer is moderate, an Au atomic percentage of around 1% is calculated outside of diffusion channels (zone 2, located ~10 nm above the GaN/Ni interface), and up to 7% locally, in such channels (zone 3). The situation is different closer to the GaN/Ni interface, where Au incorporation reaches 17% on average (zone 1, 0.7 nm wide, located ~1.4 nm above the GaN surface), confirming the Au accumulation at the GaN interface, qualitatively deduced from the relative distribution of Au in the EDX map.

The most striking result is the Ga out-diffusion detected in zones 5, 6, and 7. Au diffusion into the Ni initial layer is strong in

TABLE III. Average composition for sample B—Thick metal layers, annealed for 2 min at 450 °C in O_2 ambient (HAADF TEM image: Fig. 4).

Corresponding figure	4(b)				4(c)				4(e)	
Box positions located in the EDX map	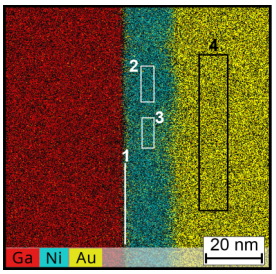				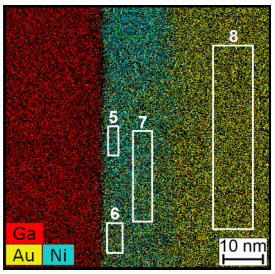				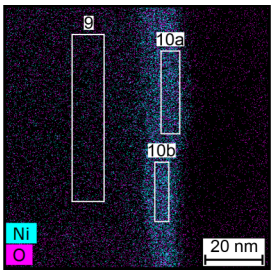	
	Average atomic percentage (%) in each box[a]									
Elements	1	2	3	4	5	6	7	8	9	10a + 10b
Ni	51.5	91.3	90.5	6.3	72.5	41.3	54.5	6.8	3.9	37.5
Au	17.4	1.2	6.9	92.1	20.8	45.2	42.0	91.3	94.9	0.1[b]
Ga	16.9	1.6	2.1	1.6	6.7	13.5	3.5	1.9	1.2	1.1
O	14.2[c]	5.9	0.4	×[d]	×[d]	×[d]	×[d]	×[d]	×[d]	61.3

[a]The TEM slice thickness is fixed to 200 nm, and the value of the material density fixed in each zone is of 19 g/cm^3 for an Au-rich zone, 9 g/cm^3 in Ni-rich zones, and 6 g/cm^3 in the NiO_x top layer.
[b]Au is only present as traces and close to the spectrum background level.
[c]This value is overestimated by more than 2%–3%. See the supplementary material.
[d]Oxygen percentage calculation from EDX is impossible in Au-rich regions. See the supplementary material.

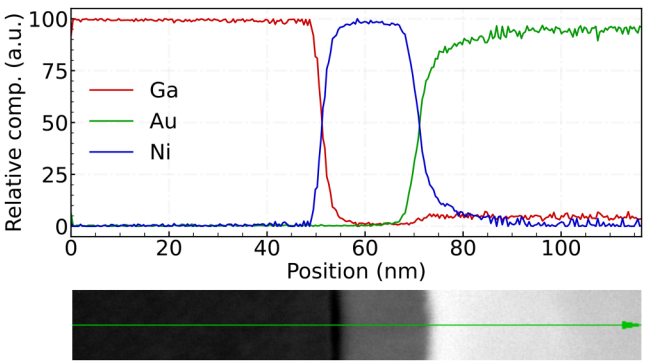

FIG. 5. Sample A (thick metal layers, non-annealed)—Relative compositional profile for Ga, Au, and Ni retrieved from EDX spectra fitting along the linescan highlighted as a green line in the bottom HAADF-STEM image.

this region, with Au incorporation up to 40% in zone 7 located ∼12 nm above the GaN/Ni. At this distance, the Ga incorporation (3.5%) is slightly larger than that expected from Ga FIB pollution at the slice facets, but still at a low level. In contrast, Ga incorporation is larger than 6% and up to 14% in zones 5 and 6 closer to the GaN/metal interface (at ∼3 nm from the interface). Considering the spatial resolution of the EDX analysis estimated to be ∼1–2 nm, this level of Ga incorporation implies Ga out-diffusion from the GaN starting during annealing, especially in regions where Au accumulation is strong.

Relative compositional profiles (EDX linescan) for Ga, Au, and Ni are reported in Figs. 5 and 6 for the non-annealed sample A and annealed (2 min—450 °C) sample B, respectively. Figure 6(a) corresponds to a region where Au diffusion is weak (Ni-rich), while Fig. 6(b) corresponds to a zone showing stronger Au diffusion. Au accumulation in the initial Ni layer and close to the GaN interface after annealing is confirmed from the profiles. Ga–Au mixing may be identified in Fig. 6(b). The direct comparison with Fig. 5 is difficult since a ∼2.9 nm thick oxide is present at the GaN/Ni interface before annealing, creating an intermediate Ga–Ni–O layer.

It can be concluded that annealing under O_2 ambient activates Ni diffusion up to the surface, where it is instantaneously oxidized. The Ni diffusion process takes place through the 200 nm thick Au layer for annealing times as short as 2 min. Ni constant oxidation at the surface seems to be crucial in promoting the diffusion process; indeed, the same thermal annealing procedure at 450 °C repeated under pure N_2 ambient for annealing times from 2 to 10 min does not improve the I–V characteristics of the contact, and Ni diffusion has not been detected on EDX maps and HR-STEM images (Fig. S1 in the supplementary material). Ni diffusion is accompanied by Au diffusion into the initial Ni layer down to the GaN surface, thereby possibly reconstructing or "auto-cleaning" the GaN/metal interface. More importantly, Ga out-diffusion from GaN is clearly ignited after 2 min of annealing and seems to be more pronounced in regions where Au accumulation is strong. Such an out-diffusion process may create Ga vacancies in the p-GaN.

Figure 7 shows an EDX linescan performed on sample C, after RTA for 10 min at 450 °C under O_2 ambient. Ni has completely

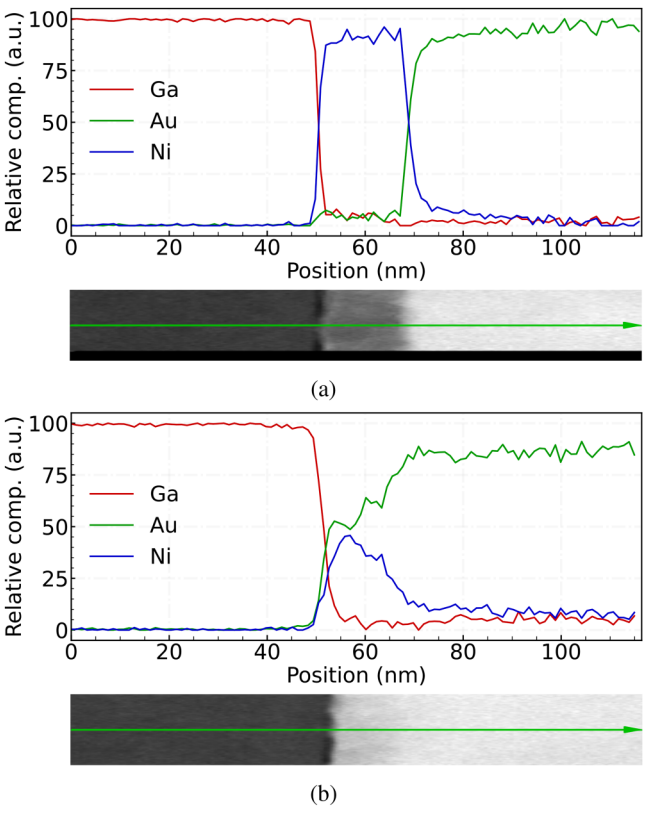

FIG. 6. Sample B (thick metal layers, annealed 2 min at 450 °C)—Relative compositional profile for Ga, Au, and Ni retrieved from EDX spectra fitting along the linescan highlighted as a green line in the bottom HAADF-STEM image. (a) In a Ni-rich region [equivalent of Fig. 4(b)] and (b) in a Au-rich region [equivalent of Fig. 4(c)].

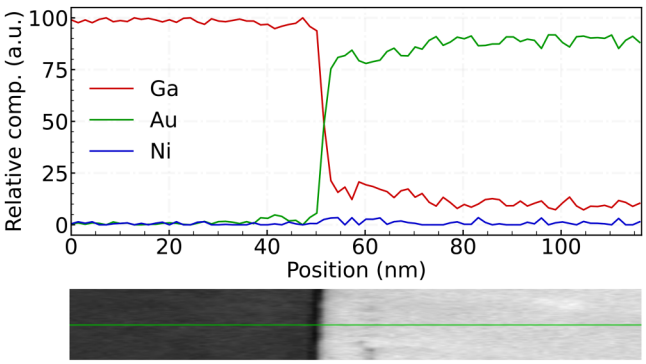

FIG. 7. Sample C (thick metal layers, annealed 10 min at 450 °C)—Relative compositional profile for Ga, Au, and Ni retrieved from EDX spectra fitting along the linescan highlighted as a green line in the bottom HAADF-STEM image.

disappeared from the GaN surface and fully diffused to the top surface. EDX analysis shows that it is fully oxidized. This is confirmed by the Z-contrast HAADF-STEM image in the bottom of Fig. 7: only a weak trace of the initial Ni/Au interface position before annealing is still visible. On the other hand, Au has fully diffused down to the GaN surface. Moreover, Ga out-diffusion is also detected with a Ga-signal in the metal layers, larger than the background level by comparison with Fig. 5. The TLM data of Fig. 2 and Table I show that the electrical results obtained after 10 min RTA are slightly improved, but close to that obtained after 2 min RTA. It is concluded that the absence of Ni, or of NiO_x at the GaN/metal interface, does not modify the ohmic behavior of the contact. Therefore, the presence of Ni/NiO_x at the GaN/metal interface is not the main origin of the contact improvement, in our case, contrary to what was supposed in previous reports.[14,16] Our results, rather, confirm that an auto-cleaning effect during interdiffusion[9,18,19] and/or the creation of Ga vacancies close to the interface[20–22] are the most probable origins of the contact improvement. It should, however, be noted that the metal adhesion to the GaN surface has been degraded after 10 min RTA, compared to the 2 min RTA for which no adhesion issue has been detected. A weak adhesion after important Au interdiffusion has already been reported by Smith *et al.*[28] Practically, a not-too-long annealing time, typically of 2–5 min in our case, seems preferable.

In order to clarify the importance of Ga out-diffusion into Au/Ni and hence the creation of Ga vacancies in the GaN layer, experiments have been repeated with thinner Ni and Au layers in order to improve the resolution of the analysis. A 3 nm thick Ni layer topped by a 3 nm thick Au layer have been evaporated onto three additional samples. The experimental protocol is identical to that presented in the beginning, except for the evaporation rate. It is reduced to 0.1 nm/s for both Ni and Au in order to get better thickness control.

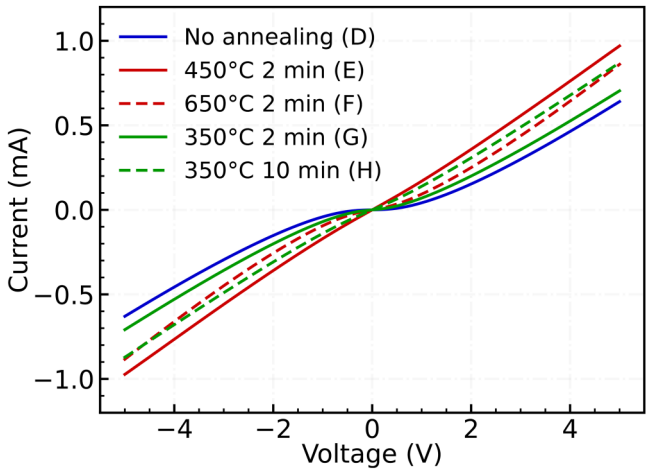

FIG. 8. TLM I–V characteristics measured for a distance between pads $L_i = 20\,\mu$m without annealing (blue), after annealing for 2 min at 450 °C (red), after annealing for 2 min at 650 °C (red dashed), after annealing at 350 °C for 2 min (green), and for 10 min (green dashed). Labels D–H refer to Table I.

Figure 8 compares the TLM I–V curves for a distance between TLM pads $L_i = 20\,\mu$m before annealing (sample D), after annealing at 450 °C for 2 min (E), at 650 °C for 2 min (F), and at 350 °C for 2 min (G), and 10 min (H). The calculated values of r_c, I_{max}, and Φ_B are listed in Table I for each sample.

Comparing the TLM curves of Figs. 2 and 8 and the results of Table I for the non-annealed samples (A and D) with thick and thin evaporated metal layers, respectively, it is first noted that the ohmic behavior is notably improved with the thin layers. Φ_B is decreased by 130 meV, while I_{max} is increased by a factor of two, and the resulting value of r_c is reduced by a factor of 10. This improvement is attributed to the lower evaporation rate, rather than to the thinner Ni and Au layers, as will be evidenced later from the HR-STEM images and EDX analysis. RTA under O_2 ambient at 450 °C for 2 min leads to a reduced Schottky barrier height and a higher I_{max} value as shown in Fig. 8. Considering Φ_B and I_{max} values, the results after annealing are close to the ones of Fig. 2 obtained for thick metal layers under same annealing conditions. The Schottky barrier has been apparently completely suppressed in the I–V curve of Fig. 8 after annealing at 450 °C for 2 min, leading to the smallest value in Table I. Although not shown, intermediate annealing tests for 2 min at 500 °C and 550 °C do not modify significantly the TLM characteristics and TLM results. RTA for 2 min at a high temperature of 650 °C starts to significantly degrade the contact. The contact between the metal surface and the electrical probes has been found to be highly resistive and non-reproducible after such annealing; a second, non-annealed, Ni–Au recharge onto the TLM pads should be evaporated for reproducible and uniform TLM measurements. The results after recharge evaporation are shown in Fig. 8.

Considering the good results already obtained after RTA for 2 min at 450 °C, it is practically more interesting to verify if a similar improvement can be obtained at a lower thermal budget. Indeed, as illustrated in Fig. 8 and in Table I, a low Schottky barrier height and a high I_{max} value can be obtained at an annealing temperature of 350 °C for an annealing time of 10 min. Generally, it can be observed from the results of Table I that the specific contact resistance is larger for the thin Ni/Au layers than for the thick Ni/Au layer. We attribute this result, rather, to the more difficult contacting with the electrical probes in the case of thin layers than to the GaN/metal contact resistance itself. A metal recharge may improve the retrieved r_c value. As a practical conclusion from the electrical characterizations, a thin Ni layer completed by an Au layer, annealed at a moderate temperature (~350 °C) under O_2 ambient, is sufficient to optimize the p-GaN/metal contact, and a low evaporation rate promotes the mechanisms in-play to form the ohmic contact, even without annealing, a result that has not been reported yet for non-alloyed Ni–Au contacts to the best of our knowledge.

Figure 9 shows a HAADF HR-STEM image of the GaN/Ni/Au stack before annealing and the corresponding EDX maps showing the relative distributions of Ga, Au, and Ni atoms. The EDX map combining Ga, Ni, and Au relative distributions is given as an insert in Table IV. From the Z-contrast of Fig. 9(a), the measured average thickness of the two metal layers is of 2.7 ± 0.1 and

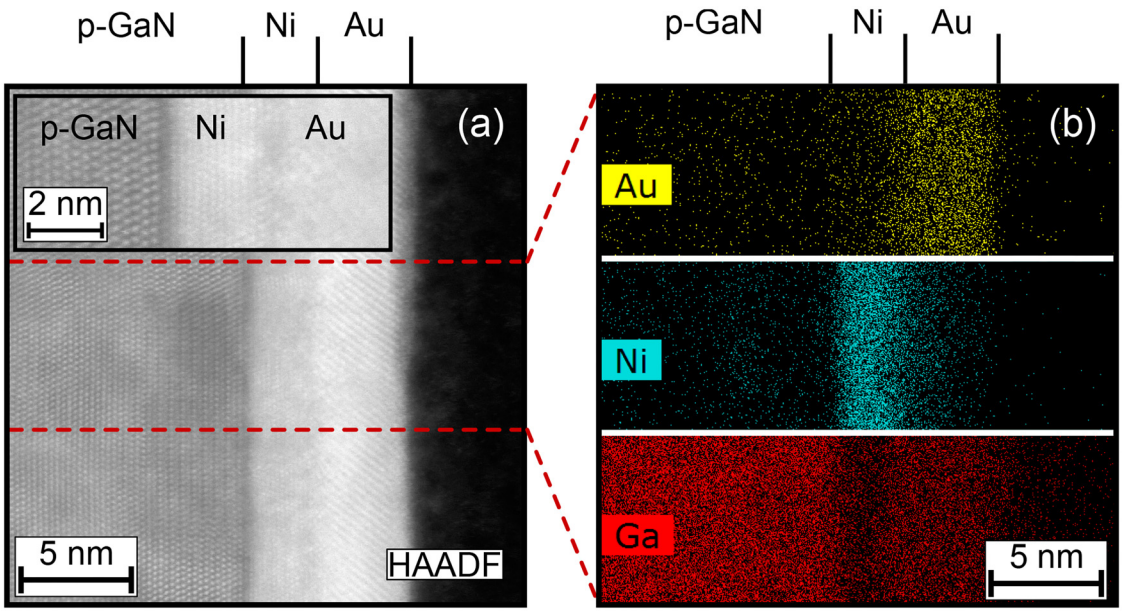

FIG. 9. Sample D (thin metal layers, non-annealed): (a) HR-STEM image and (b) EDX maps showing the relative distribution of Ga, Ni, and Au atoms. The inset in (a) is a higher-magnification HAADF-STEM image of the GaN/Ni/Au interfaces. The interval between the horizontal red dashed lines in the HAADF image corresponds to the same analyzed area in the EDX maps, vertically spaced.

2.8 ± 0.1 nm, close to the nominal value of 3 nm. Although not shown, the GaN/Ni interface is found to be uniform at a larger-scale, and the Ni layer is nano-crystallized as evidenced in the inset of Fig. 9(a). A very thin (<0.5 nm) layer of lower density (appearing as dark in the HAADF image), presumably an oxide, is only present in localized and discontinuous regions of the GaN/Ni interface.

It could, therefore, be inferred that this sample is close to the ideal p-GaN/Ni diode for which a moderate Schottky barrier height is theoretically expected,[4,6,7] which might explain the better electrical results obtained in comparison with the non-annealed sample with thicker metal layers evaporated at a high rate. On the other hand, despite the absence of annealing, Fig. 9(b) evidences that a diffusion process has already started to take place. An overlap between the Au and Ni signals is visible when comparing the top and middle EDX maps. The most striking result deals with the Ga atom distribution, which spreads over the initial Ni and Au layers where its relative intensity is much higher than that typically attributed to Ga FIB pollution. A more quantitative analysis of the composition in atomic percentage for sample D has been carried out in three rectangular areas selected in the initial Ni layer, the Au layer, and the top of the Au layer, following the same approach as in Fig. 3(b). The positions of the rectangular areas are shown in the inset image of Table IV, summarizing the obtained results. Ni is predominant in zone 1, but Au and Ga are also present. The oxygen concentration is overestimated in this relatively dense layer for the reason explained in the supplementary material; the situation is at the limit case where oxygen concentration can be retrieved in a reliable manner from the TEM-EDX technique. The diffusion of Ga into Ni and Au corresponds to an average Ga composition in atomic percentage in the selected zones 1 and 2 above 14%, and Ga accumulation is evidenced on the top part of the Au layer in zone 3, where an average Ga composition of 30% is

TABLE IV. Average composition for sample D—Thin metal layers, non-annealed (HAADF TEM image: Fig. 9).

Box positions located in the EDX map	Element	Average atomic % in each zone[a]		
		1	2	3
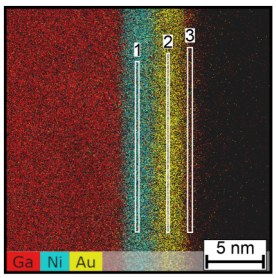	Ni	67.3[b]	16.7	1.2
	Au	5.3[b]	65.1	8.8
	Ga	14.4[b]	18.2	30.3
	O	13.2[c]	×[d]	59.7

[a]The TEM slice thickness is fixed to 200 nm, and the average material density is fixed to 8 g/cm^3 for zone 1 and 15 g/cm^3 for zones 2 and 3.
[b]The at. % calculated in the limit case where oxygen is discarded from the volume is Ni% = 77.3%, Au% = 6.1%, and Ga% = 16.6%.
[c]This value is overestimated by more than 2%–3%. See the supplementary material.
[d]Oxygen percentage calculation from EDX is impossible in Au-rich regions. See the supplementary material.

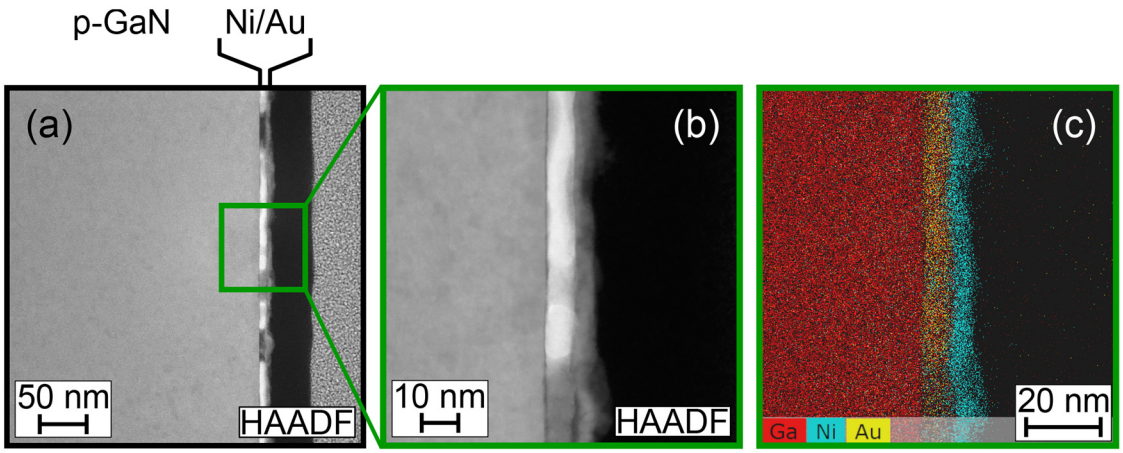

FIG. 10. Sample E (thin metal layers, annealed 2 min at 450 °C): (a) Large-scale HAADF HR-STEM image, (b) higher-magnification HAADF-STEM image, and (c) the corresponding EDX map showing the superimposed relative distributions of Ni (blue), Ga (red), and Au (yellow) atoms.

calculated. Considering the spatial resolution of our EDX analysis, estimated to be of at most 2 nm (mostly due to some possible image drift during the acquisition), such percentages cannot be only inferred to an artifact in the EDX analysis due to the too closely spaced interfaces.

At this extreme surface, gallium is oxidized as deduced from the oxygen percentage. Although not shown, average Ga composition in atomic percentage up to 25% and 30% has been calculated at a different position of the TEM slice in the Ni layer and the Au layer, respectively. This level is much higher than the one due to possible Ga-pollution. Moreover, in crystallized, Ga-rich, interdiffused Au–Ga zones, the inter-planar spacing (0.333 nm) retrieved from the fast Fourier transform of TEM images is significantly different from inter-planar spacing values expected for a pure fcc gold crystal (smaller than 0.240 nm) confirming the presence of Ga in the volume and not only at the slice facets.

The main origin for the onset of the Ni, Au, and Ga diffusion process without any thermal annealing still needs clarification. Ga diffusion up to the Au layer might have started *in situ* during metal evaporation, considering the low evaporation rate and the very thin Ni layer, which does not act as an efficient diffusion barrier. It may also have been ignited in ambient air, after deposition, facilitated by the small thickness (<3 nm) of the metal layers and assisted by the presence of oxygen. As an important conclusion of these experimental observations, whatever its origin, the Ga diffusion process must have created Ga vacancies in GaN close to the GaN/metal interface. It is, therefore, likely that the Ga vacancies play a crucial role in the improved electrical behavior of the TLM contacts in Fig. 8 even before annealing. Our assumption is consistent with the results of Jang *et al.*,[20] showing that the modifications of the GaN surface subsequent to thermal annealing of the Ni/Au contact and exo-diffusion of Ga into Au are a crucial mechanism to obtain an ohmic-like p-GaN contact.

Figure 10(a) shows a large-scale, HR-STEM image of the GaN/Ni/Au stack at a higher magnification, after RTA under an O_2 atmosphere at 450 °C for 2 min. As reported in Fig. 8 and Table I, the electrical contact is improved after such annealing. The Ni–Au region appears non-uniform at the nano-scale, with some bright and dark areas in the Z-contrast HAADF image. Dark areas may be attributed to intergranular nano-voids embedded in the TEM slice thickness, formed during the annealing at 450 °C. Figure 10(b) shows a higher-magnification HAADF HR-STEM image at a frontier between dark/light areas, marked with a green square in Fig. 10(a), and the corresponding EDX map with the superimposed relative distributions of Ga, Ni, and Au atoms, used for quantitative analyses of the atomic composition, is shown in Fig. 10(c). The EDX map with the superimposed relative distributions of Ni and O atoms, showing the three zones selected for the analysis, is reported as an inset in Table V, summarizing the calculated atomic percentages in the different zones.

It can be concluded from the results of Table V that, as for the case of 20/200 nm Ni/Au layers, annealing in an O_2 atmosphere has promoted the diffusion of Ni on top of the Au layer, where it is fully oxidized with a Ni/O ratio close to 1, while Au has diffused down to the GaN surface replacing Ni, and almost no trace of Au is detected anymore at the top surface. The Ni–Au inter-diffusion process is almost complete after 2 min at 450 °C, to be related to the small metal layer thicknesses. Moreover, TEM observations at the highest magnification show that the thin layers are mostly crystallized at the nano-scale, including the NiO_x top layer. In parallel, Ga atoms' out-diffusion into the Au layer has been strongly reinforced during RTA, with more than 60% of Ga (in atomic percentage) now incorporated, forming an Au–Ga alloy with Ni nano-crystallites, probably creating more Ga vacancies in the GaN layer. Detecting vacancies in a GaN crystal is beyond the resolution of our TEM-EDX analysis, as illustrated by a line profile in Fig. S2 of the supplementary material. Further investigation and different physico-chemical analysis are required to this aim. Finally, it can be noted that the average compositions in atomic percentages retrieved for zone 1 (selected in a bright region of the Z-contrast

TABLE V. Average composition for sample E—Thin metal layers, annealed for 2 min at 450 °C in O_2 ambient (HAADF TEM image: Fig. 10).

Box positions located in the EDX map	Element	Average atomic % in each zone[a]		
		1	2	3
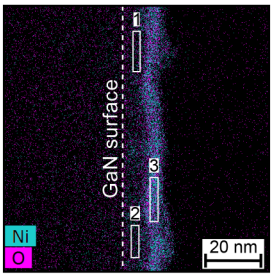	Ni	9.0	16.2	46.6
	Au	22.0	16.0	0[b]
	Ga	69.0	67.8	5.1
	O	×[c]	×[c]	48.4

[a]The TEM slice thickness is fixed to 100 nm, and the average material density is fixed to 10 g/cm^3 for zones 1 and 2 and 7 g/cm^3 for zone 3.
[b]Calculated value, no Au signal in the EDX spectrum.
[c]Oxygen percentage calculation from EDX is impossible in Au-rich regions. See the supplementary material.

HAADF image) and for zone 2 (selected in a dark region of the Z-contrast HAADF image) are similar, indicating that the change in the intensity is rather due to some nano-domains and nano-voids formed during the annealing at 450 °C in the thin alloy and embedded in the thickness of the TEM slice, rather than to a change in composition.

TEM observations and EDX analysis after annealing at 650 °C for 2 min showed the same composition; however, it was observed that the Au–Ga layer on top of the GaN surface is discontinuous, with large voids clearly apparent on the HAADF images, as can be seen in Fig. S3 of the supplementary material. This may explain the difficulty in contacting the TLM pad surface with the electrical probes reported above. Our STEM-EDX experimental observations, combined with the results of Figs. 2 and 8 and of Table I, confirm that the creation of Ga vacancies should play a crucial role in forming an ohmic-like p-GaN/metal contact in our processing conditions. It is also clearly evidenced that neither Ni nor NiO_x is necessarily in contact with p-GaN to obtain such a result. Rather, a p-GaN/Ga–Au layer seems beneficial to the improvement of the electrical characteristics. We, therefore, support the conclusion that creating Ga vacancies represents the key-mechanism to obtain a ohmic contact on p-doped GaN. Our STEM-EDX analysis also explains why removing chemically the NiO_x layer after the RTA step, as proposed by Mengzhe *et al.*,[29] does not degrade the electrical properties of p-GaN/metal contact.

IV. CONCLUSION

We have investigated in detail the formation of an ohmic contact on p-GaN using a Ni–Au metal layer. We confirm that an O_2 atmosphere during post-deposition thermal annealing is determinant to decrease the Schottky barrier height and to improve the contact ohmicity since oxygen assists the Ni–Au inter-diffusion process during annealing, with Ni being immediately oxidized when reaching the top surface. More interestingly, our results demonstrate that the presence of NiO_x in contact with GaN is not required to improve the ohmic behavior of the contact, in contrast with a recent report. A GaN/Au–Ga interface leads to better electrical results than a GaN/NiO_x interface. We evidence that Ga out-diffusion accompanying the Au–Ni interdiffusion process to form a Ga-rich, Au–Ga alloy plays a key-role to create Ga vacancies in the p-GaN. The best electrical results are obtained in such conditions, and we presume that the creation of Ga vacancies in the top p-GaN surface is the most crucial mechanism in order to obtain an ohmic contact.

SUPPLEMENTARY MATERIAL

See the supplementary material for detailed information regarding the epitaxial structure, processing steps, electrical characterization, FIB etching, and TEM-EDX analysis.

ACKNOWLEDGMENTS

The authors thank Francesco Daddi of Grenoble INP Phelma, France for taking part in TLM characterizations and Hannah Lias of South Dakota School of Mines and Technology, USA for proof-reading the manuscript during their internship in the C2N laboratory. Part of this work was supported by ANR project CORTIORGAN (No. ANR-22-CE08-0020-03), and ANR project NEWAVE (No. ANR-21-CE24-0019-04). C2N and IEMN are members of RENATECH, the national network of large academic micro-nanofabrication facilities. FIB equipment co-funding: CPER Hauts de France project IMITECH and the Métropole Européenne de Lille.

AUTHOR DECLARATIONS

Conflict of Interest

The authors have no conflicts to disclose.

Author Contributions

Jules Duraz: Formal analysis (equal); Investigation (equal); Writing – review & editing (equal). **Hassen Souissi:** Investigation (equal); Writing – review & editing (equal). **Maksym Gromovyi:** Investigation (equal); Writing – review & editing (equal). **David Troadec:** Resources (equal). **Téo Baptiste:** Resources (supporting). **Géraldine Hallais:** Investigation (equal). **Nathaniel Findling:** Resources (supporting). **Phuong Vuong:** Resources (equal). **Rajat Gujrati:** Resources (supporting). **Thi May Tran:** Resources (supporting). **Jean-Paul Salvestrini:** Funding acquisition (equal); Resources (equal). **Maria Tchernycheva:** Funding acquisition (equal); Writing – review & editing (equal). **Suresh Sundaram:** Resources (equal). **Abdallah Ougazzaden:** Funding acquisition (equal); Resources (equal). **Gilles Patriarche:** Investigation (equal); Writing – review & editing (equal). **Sophie Bouchoule:** Funding acquisition (equal); Supervision (equal); Writing – original draft (equal); Writing – review & editing (equal).

DATA AVAILABILITY

The data that support the findings of this study are available from the corresponding author upon reasonable request.

REFERENCES

[1]M. Hiroki, K. Kumakura, Y. Kobayashi, T. Akasaka, T. Makimoto, and H. Yamamoto, "Suppression of self-heating effect in AlGaN/GaN high electron mobility transistors by substrate-transfer technology using h-BN," Appl. Phys. Lett. **105**, 193509 (2014).

[2]J. Shin, H. Kim, S. Sundaram, J. Jeong, B.-I. Park, C. S. Chang, J. Choi, T. Kim, M. Saravanapavanantham, K. Lu, S. Kim, J. M. Suh, K. S. Kim, M.-K. Song, Y. Liu, K. Qiao, J. H. Kim, Y. Kim, J.-H. Kang, J. Kim, D. Lee, J. Lee, J. S. Kim, H. E. Lee, H. Yeon, H. S. Kum, S.-H. Bae, V. Bulovic, K. J. Yu, K. Lee, K. Chung, Y. J. Hong, A. Ougazzaden, and J. Kim, "Vertical full-colour micro-LEDs via 2D materials-based layer transfer," Nature **614**, 81–87 (2023).

[3]J. Chen and W. D. Brewer, "Ohmic contacts on p-GaN," Adv. Electron. Mater. **1**, 1500113 (2015).

[4]G. Greco, F. Iucolano, and F. Roccaforte, "Ohmic contacts to gallium nitride materials," Appl. Surf. Sci. **383**, 324–345 (2016).

[5]B. Ofuonye, J. Lee, M. Yan, C. Sun, J.-M. Zuo, and I. Adesida, "Electrical and microstructural properties of thermally annealed Ni/Au and Ni/Pt/Au Schottky contacts on AlGaN/GaN heterostructures," Semicond. Sci. Technol. **29**, 095005 (2014).

[6]K. A. Rickert, A. B. Ellis, J. K. Kim, J.-L. Lee, F. J. Himpsel, F. Dwikusuma, and T. F. Kuech, "X-ray photoemission determination of the Schottky barrier height of metal contacts to n–GaN and p–GaN," J. Appl. Phys. **92**, 6671–6678 (2002).

[7]S. Wahid, N. Chowdhury, M. K. Alam, and T. Palacios, "Barrier heights and Fermi level pinning in metal contacts on p-type GaN," Appl. Phys. Lett. **116**, 213506 (2020).

[8]H. K. Cho, T. Hossain, J. W. Bae, and I. Adesida, "Characterization of Pd/Ni/Au ohmic contacts on p-GaN," Solid-State Electron. **49**, 774–778 (2005).

[9]J.-L. Lee, J. K. Kim, J. W. Lee, Y. J. Park, and T. Kim, "Effect of surface treatment by KOH solution on ohmic contact formation of p-type GaN," Solid-State Electron. **43**, 435–438 (1999).

[10]J.-S. Jang, S.-J. Park, and T.-Y. Seong, "High quality non-alloyed Pt ohmic contacts to p-type GaN using two-step surface treatment," MRS Internet J. Nitride Semicond. Res. **5**, 521–527 (2000).

[11]L. Zhou, W. Lanford, A. T. Ping, I. Adesida, J. W. Yang, and A. Khan, "Low resistance Ti/Pt/Au ohmic contacts to p-type GaN," Appl. Phys. Lett. **76**, 3451–3453 (2000).

[12]C. Huh, S.-W. Kim, H.-M. Kim, D.-J. Kim, and S.-J. Park, "Effect of alcohol-based sulfur treatment on Pt ohmic contacts to p-type GaN," Appl. Phys. Lett. **78**, 1942–1944 (2001).

[13]J. K. Sheu, Y. K. Su, G. C. Chi, W. C. Chen, C. Y. Chen, C. N. Huang, J. M. Hong, Y. C. Yu, C. W. Wang, and E. K. Lin, "The effect of thermal annealing on the Ni/Au contact of p-type GaN," J. Appl. Phys. **83**, 3172–3175 (1998).

[14]J.-K. Ho, C.-S. Jong, C. C. Chiu, C.-N. Huang, C.-Y. Chen, and K.-K. Shih, "Low-resistance ohmic contacts to p-type GaN," Appl. Phys. Lett. **74**, 1275–1277 (1999).

[15]D. Mistele, F. Fedler, H. Klausing, T. Rotter, J. Stemmer, O. K. Semchinova, and J. Aderhold, "Investigation of Ni/Au-contacts on p-GaN annealed in different atmospheres," J. Cryst. Growth **230**, 564–568 (2001).

[16]L.-C. Chen, F.-R. Chen, J.-J. Kai, L. Chang, J.-K. Ho, C.-S. Jong, C. C. Chiu, C.-N. Huang, C.-Y. Chen, and K.-K. Shih, "Microstructural investigation of oxidized Ni/Au ohmic contact to p-type GaN," J. Appl. Phys. **86**, 3826–3832 (1999).

[17]T. Maeda, Y. Koide, and M. Murakami, "Effects of NiO on electrical properties of NiAu-based ohmic contacts for *p*-type GaN," Appl. Phys. Lett. **75**, 4145–4147 (1999).

[18]D. Qiao, L. S. Yu, S. S. Lau, J. Y. Lin, H. X. Jiang, and T. E. Haynes, "A study of the Au/Ni ohmic contact on p-GaN," J. Appl. Phys. **88**, 4196–4200 (2000).

[19]Y. Koide, T. Maeda, T. Kawakami, S. Fujita, T. Uemura, N. Shibata, and M. Murakami, "Effects of annealing in an oxygen ambient on electrical properties of ohmic contacts to p-type GaN," J. Electron. Mater. **28**, 341–346 (1999).

[20]H. W. Jang, S. Y. Kim, and J.-L. Lee, "Mechanism for ohmic contact formation of oxidized Ni/Au on p-type GaN," J. Appl. Phys. **94**, 1748–1752 (2003).

[21]J. K. Kim, J. H. Je, J.-L. Lee, Y. J. Park, and B.-T. Lee, "Microstructural investigation of Ni/Au ohmic contact on p-type GaN," J. Electrochem. Soc. **147**, 4645 (2000).

[22]B. Sarkar, P. Reddy, A. Klump, F. Kaess, R. Rounds, R. Kirste, S. Mita, E. Kohn, R. Collazo, and Z. Sitar, "On Ni/Au alloyed contacts to Mg-doped GaN," J. Electron. Mater. **47**, 305–311 (2018).

[23]C. Mauduit, T. S. Tlemcani, M. Zhang, A. Yvon, N. Vivet, M. Charles, R. Gwoziecki, and D. Alquier, "Importance of layer distribution in Ni and Au based ohmic contacts to p-type GaN," Microelectron. Eng. **277**, 112020 (2023).

[24]G. Greco, P. Prystawko, M. Leszczyński, R. Lo Nigro, V. Raineri, and F. Roccaforte, "Electro-structural evolution and Schottky barrier height in annealed Au/Ni contacts onto p-GaN," J. Appl. Phys. **110**, 123703 (2011).

[25]G. K. Reeves and H. B. Harrison, "Obtaining the specific contact resistance from transmission line model measurements," IEEE Electron Device Lett. **3**, 111–113 (1982).

[26]T. Mori, T. Kozawa, T. Ohwaki, Y. Taga, S. Nagai, S. Yamasaki, S. Asami, N. Shibata, and M. Koike, "Schottky barriers and contact resistances on p-type GaN," Appl. Phys. Lett. **69**, 3537–3539 (1996).

[27]R. T. Tung, "The physics and chemistry of the Schottky barrier height," Appl. Phys. Rev. **1**, 011304 (2014).

[28]L. L. Smith, R. F. Davis, M. J. Kim, R. W. Carpenter, and Y. Huang, "Microstructure, electrical properties, and thermal stability of Au-based ohmic contacts to p-GaN," J. Mater. Res. **12**, 2249–2254 (1997).

[29]L. Mengzhe, C. Qing, Y. Tingjing, Z. Shuming, and C. Lianghui, "NiO removal of Ni/Au ohmic contact to p-GaN after annealing," J. Semicond. **30**, 026001 (2009).